Key Engineering Materials
ISSN: 1662-9795, Vol. 926, pp 655-662
doi:10.4028/p-232uip

Submitted: 2021-11-30
Revised: 2022-02-03
Accepted: 2022-02-08
Online: 2022-07-22

Setting Residual Stresses in Tensile Stress-Superposed Incremental Sheet Forming

F. Maaß[1,a,*], M. Hahn[1,b] and A.E. Tekkaya[1,c]

[1]Institute of Forming Technology and Lightweight Components, TU Dortmund University, Baroper Str. 303, 44227 Dortmund, Germany

[a]fabian.maass@iul.tu-dortmund.de; [b]marlon.hahn@iul.tu-dortmund.de; [c]erman.tekkaya@iul.tu-dortmund.de

Keywords: Incremental forming, stress superposition, residual stress

Abstract. Incremental sheet metal sheet forming (ISF) is a flexible forming process to manufacture sheet metal parts. ISF processes allow a control of residual stresses depending on the process parameters and the acting forming mechanisms. These forming-induced residual stresses highly influence the product properties. This paper presents numerical and experimental results demonstrating the influence of biaxial tensile stress-superposed incremental forming (TSSIF) on the residual stress of truncated cones. An adjustable clamping frame is used to apply defined tensile stresses over the sheet plane in biaxial direction during forming. Residual stresses are evaluated by means of x-ray diffraction on both sides of the formed component. TSSIF influences the amplitudes of the residual stresses on both sides of the formed component. The residual stresses can be adjusted depending on the amount of initial tensile stresses in order to meet specified product properties.

Introduction

Incremental Sheet Forming. In incremental sheet metal forming (ISF) a sheet metal is formed by the continuous movement of a non-geometry dependent hemispherical forming tool while the metal sheet is clamped at the edges (**Fig. 1**). The forming tool is moved along a predefined toolpath derived from the desired CAD geometry and only a small area of the sheet is in contact with the forming tool. Due to the localized deformation zone, very high strains occur locally [1]. The advantage of the non-geometry dependent forming tool are low tooling costs and a flexible manufacturing process that is particularly suitable for small batch sizes and rapid prototyping [2]. ISF process was patented by Leszak in 1967 and includes two process groups [3]. A variant without using a supporting die and a variant with dies or supporting tools. Single Point Incremental Forming (SPIF) as described by Jeswiet et al. can be performed on conventional 3-axis CNC milling machine to produce complex parts without using partial or full dies [4]. SPIF is the most flexible ISF process occurring springback leads to competently poor geometrical accuracy. Two Point Incremental Forming (TPIF) as presented by Powell and Andrew can improve the geometrical accuracy of the manufactured components by using additional supporting tools or dies with reduced flexibility [5].

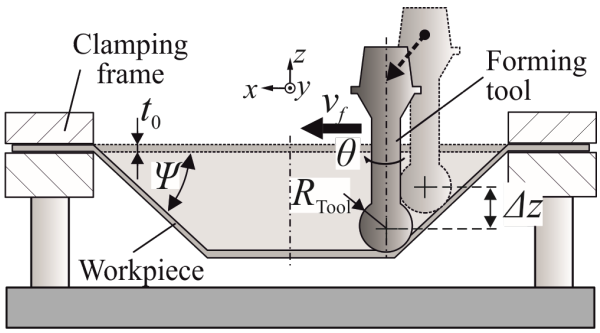

Figure 1. Single Point Incremental Forming process principal (cross-sectional view)

A common disadvantage of ISF processes is high process time compared to conventional forming processes. The process combination of ISF and stretch forming presented by Taleb Araghi et al. can

lead to a noticeable reduction of production time [6]. In a two step-process the sheet metal is stretch formed over a positive die using a servo-driven movable blank holder. After the stretch forming process, features can be formed into the pre-formed part using ISF to achieve the final part geometry. A more uniform thickness distribution with a reduced amount of maximum thinning was observed using this process combination. This approach is beneficial regarding the production time. Because of the need for geometry-dependent full dies, this approach is not beneficial in case of flexibility, especially compared to SPIF processes.

Residual stresses are inherent generated in metal components during forming processes. A control of residual stresses by means of forming processes are barely considered during the component design process. A control of residual stresses can lead to optimized component properties such as geometric accuracy and fatigue strength. In recent publications the possibility of controlling residual stresses through incremental forming processes was analyzed and proved [7]. Due to the incremental process character, the process parameters can be adjusted locally during the entire process, in contrast to conventional forming processes. The possibilities of adjusting residual stresses through the process parameters of incremental forming are limited. Approaches of stress-superposed incremental forming using flexible polymer dies to induce compressive residual stresses on both sides of manufactured truncated aluminum cones, showed the potential of setting residual stresses to meet specified product properties [8].

The objective of this paper is to provide a new approach of superpose tensile stresses over the sheet plane during incremental forming to generate tailored residual stresses. An adjustable clamping frame is introduced to apply defined tensile loaded over the sheet plane in uni- or biaxial direction. This tensile stress-superposed incremental forming (TSSIF) has the same flexibility as SPIF processes. Additionally, an adjustment of the tensile load over the sheet plane is possible during the whole forming process. Identical truncated cone geometries are manufactured by TSSIF and SPIF to compare the effect on the residual stresses as well as the process forces, geometry and material hardness of the components are analyzed.

Procedure

Tensile stress-superposition process set-up. The process set-up for tensile stress-superposed incremental forming (TSSIF) is described in **Fig. 2a**. A single point incremental forming set-up is used consisting of a forming tool R_{tool} = 15 mm and clamping frame. Instead of a ridged clamping, an adjustable clamping is added to the SPIF set-up. Two sides of the clamping can be moved by hydraulic cylinders along rails in x-direction respectively y-direction, independently. The forming area is not affected by the TSSIF set-up. The TSSIF set-up is mounted to a DMG Mori® 5-axis DMU 50 milling machine. The tool movement is carried out by the computer numerical control of the milling machine and the process forces are measured by a three-component load cell (**Fig. 2b**). Incremental forming parameters used are step-down increment Δz = 1.875 mm with rotating tool motion θ_{tool} = 300 RPM and a tool feed rate v_{tool} = 600 mm/min. Truncated cone geometries are used as reference geometries that are manufactured by laser-cut aluminum AA5083 sheet material in H111 condition with an initial sheet thickness of t_0 = 1.0 mm. The rectangular unclamped sheet area has a dimension of 205 x 205 mm. The initial diameter of the truncated geometry is D = 150 mm with a wall angle Ψ = 40°. The targeted cone height is h = 33.75 mm. Tests without tensile-stress superposition, comparable to SPIF and two separate tests with different initial biaxial stresses in sheet plane direction with $\sigma_{\text{tensile,1}}$ = 35.6 MPa that equals 21.6 % of the initial yield stress of the AA5083 material and $\sigma_{\text{tensile,2}}$ = 71.2 MPa that equals 43.2 % of the initial yield stress of the AA5083 material, are performed.

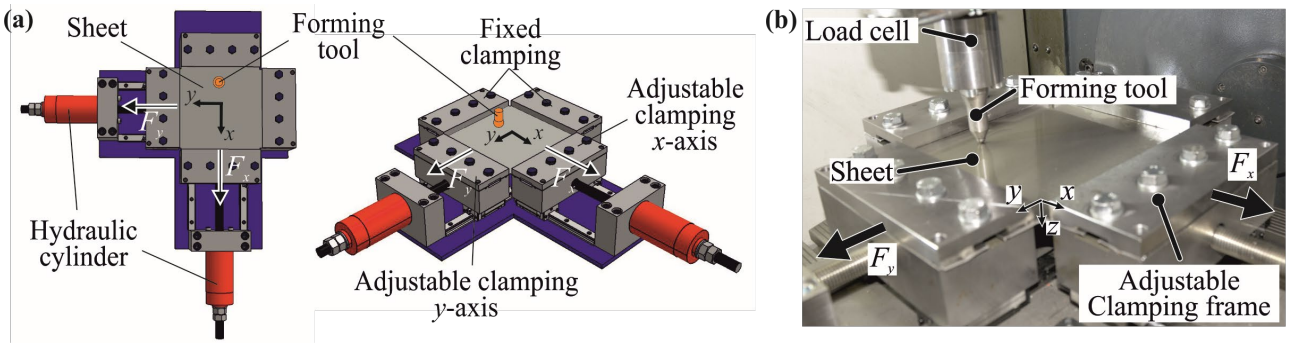

Figure 2. (a) Tensile stress-superposed incremental forming (TSSIF) process principal (b) TSSIF process set-up

Residual stress measurement. Residual stress measurements are carried out by non-destructive X-ray diffraction using a Stresstech GmbH® Xstress G2R X-ray diffractometer to measure the near-to-surface residual stresses. The strain analysis is based on the determination of the interplanar distance d{hkl} (hkl-Miller indices) according to the Bragg law in **Eq. 1**. Where n is the order of diffraction of the interference $\{hkl\}$, λ is the wavelength, and θ is its Bragg angle as decribed in **Fig. 3a**.

$$n \cdot \lambda = 2 \cdot d_{\{hkl\}} \cdot \sin\theta \tag{1}$$

The residual stresses are determined in the middle of the cone wall h_m = 16.875 mm in meridional σ_m and circumferential σ_c direction on both sides of the cone wall as shown in **Fig. 3b**. The interplanar grid spacings for different sample orientations are measured according to the tensor character of strains and stresses. The stresses are calculated using the $\sin^2\Psi$-method [9]. Co-Kα radiation with a penetration depth of τ = 5 µm is used. The 2θ angle has a range of -42° – 42° (±3° oscillation). A collimator with a spot size of 2 mm is used. The exposure time is t = 20 s per step. The reflection profiles are recorded for the 9 Ψ-inclinations (0°, ±18.7°, ±27°, ±33.8°, ±40°). The resulting stresses are mean values of three repeated measurements.

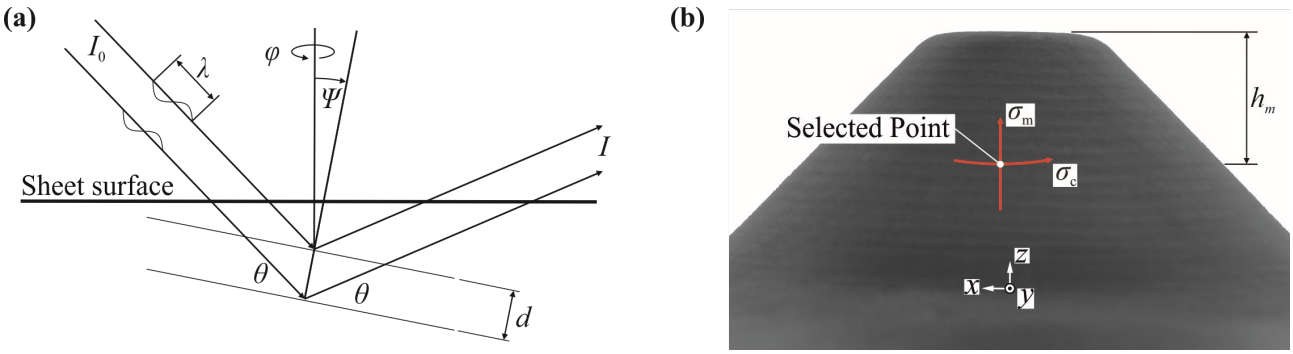

Figure 3. (a) XRD measurement method (b) Truncated cone geometry with selected measuring point

Numerical process model. A finite element model was built in ABAQUS® according to the experimental setup in **Fig. 2b**. The numerical model consists of the forming tool modeled as a rigid body and the sheet blank modelled with solid elements (C3D8I) as shown in **Fig. 4a**. The sheet blank elements have an edge length of 1 mm with five elements over the sheet thickness. The numerical model consists of three steps. In the first step, a tensile load is applied as a surface load to the edge elements of the sheet blank. The second step includes the process model that is explicitly time integrated with a time step of 1×10^{-06} s. In an implicit third step the unclamping process is numerically reproduced. The material model for the sheet metal includes combined isotropic-kinematic hardening including cyclic hardening based on Lemaitre and Chaboche [10]. A penalty contact is used for the interaction of forming tool and sheet. The AA5083 sheet metal material was characterized using uniaxial tensile tests and in-plane torsion tests. The results are shown in **Fig. 4b**. The initial yield

stress of the AA5083 material is determined to $\sigma_{y,0}$ = 165 MPa. The cyclic hardening parameters are determined inversely as Q_∞ = 83 MPa and b = 9.88 as described in [11].

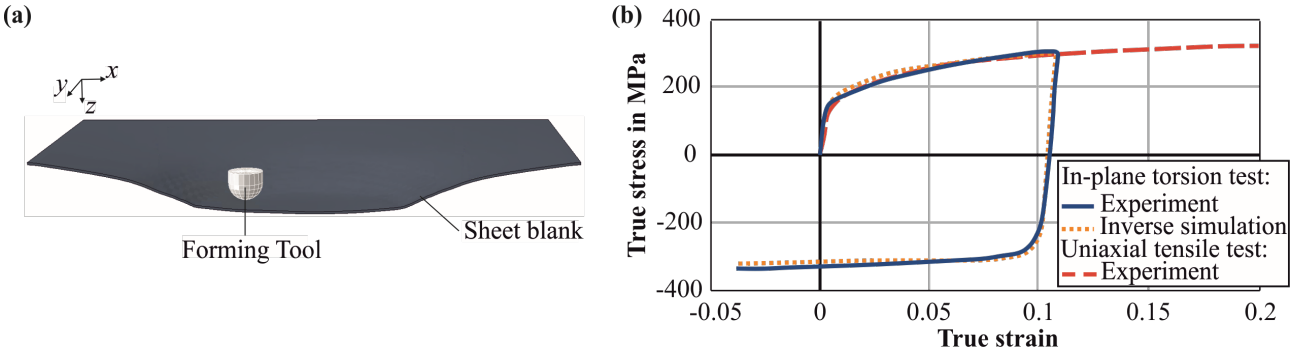

Figure 4. (a) Numerical process model set-up (b) Material characterization AA5083

Results

Process forces. The measured experimental process forces in z-direction are shown in **Fig. 5a**. Qualitatively the force development of tensile stress-superposed (TSSIF) and non-tensile stress-superposed (SPIF) processes show the same behavior during the 18 step-down increments. The maximum forming forces for all three x-, y-, z-components are shown in **Fig. 5b**. Maximum process force values are mean values of three repetitions. Maximum measured process forces F_z for all process variants are on the same level ($F_{z,\,SPIF}$ = 1,98 kN, $F_{z,\,20\%\,\sigma t}$ = 1,95 kN, $F_{z,\,40\%\,\sigma t}$ = 1,96 kN). Forming forces in x- and y-direction are 70 % smaller than the forming forces in z-direction. According to F_z, the forming forces x- and y-direction are on the same level for all process variants. The evaluated forming forces of the numerical process model in **Fig. 5b** show the same qualitative behavior comparing all three process variant. The forming forces for all component directions are an upper bound regarding the experimental results. The forming forces slightly decreases with increasing tensile stress-superposition. The forming forces in x- and y-direction are exactly the same for each process variant due to the axisymmetric process set-up. It can be concluded, that the forming forces of all process variants are almost the same.

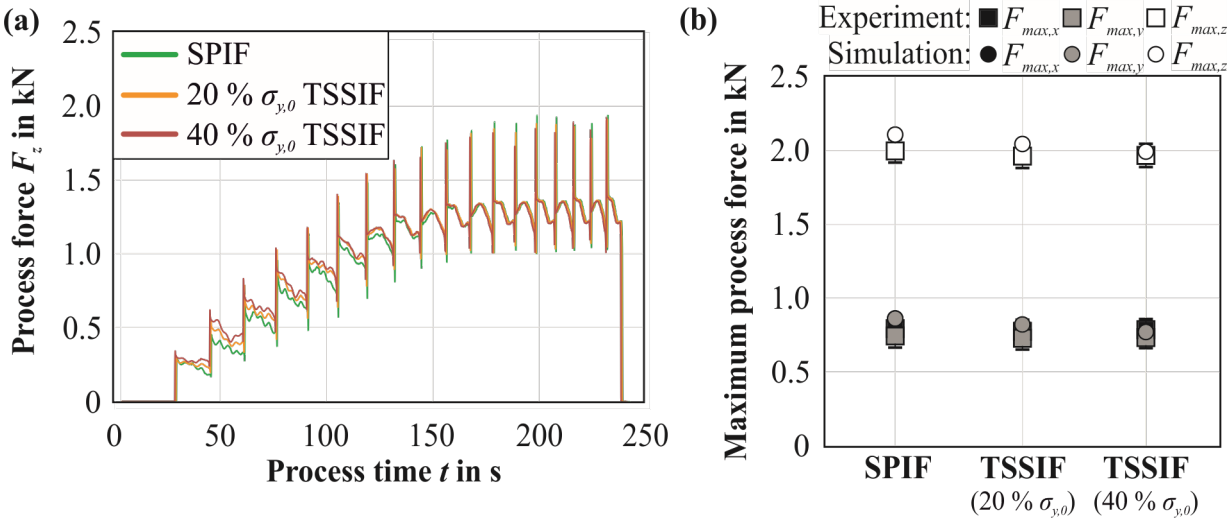

Figure 5. (a) Experimental process forces (z-direction) (b) Maximum process forces

Geometry. 3D-digitalizer GOM® ATOS II is used to digitalize and analyzing the resulting geometry of all formed cones (**Fig. 6a**). Further geometric evaluation was done using ATOS Professional V8 SR1 software. The experimental geometrical accuracy compared to an ideal (CAD) target geometry is plotted in **Fig. 6b** for SPIF and TSSIF processes. A comparison of cut A-A is representative for the whole cone geometry due to the axisymmetric characteristic of the cone

geometry. A comparison of all three process variants cut's show great conformity in the cone wall area and the bottom area of the formed cone. Regarding the flange area there are slight deviations between the process variants. Regarding the target geometry all process variants meet the target geometry in the bottom and cone wall area with slight deviations due to springback effects. The flange area shows large deviations compared to the target geometry as expected for SPIF components. The numerical results show geometrical deviations equal to the experimental results.

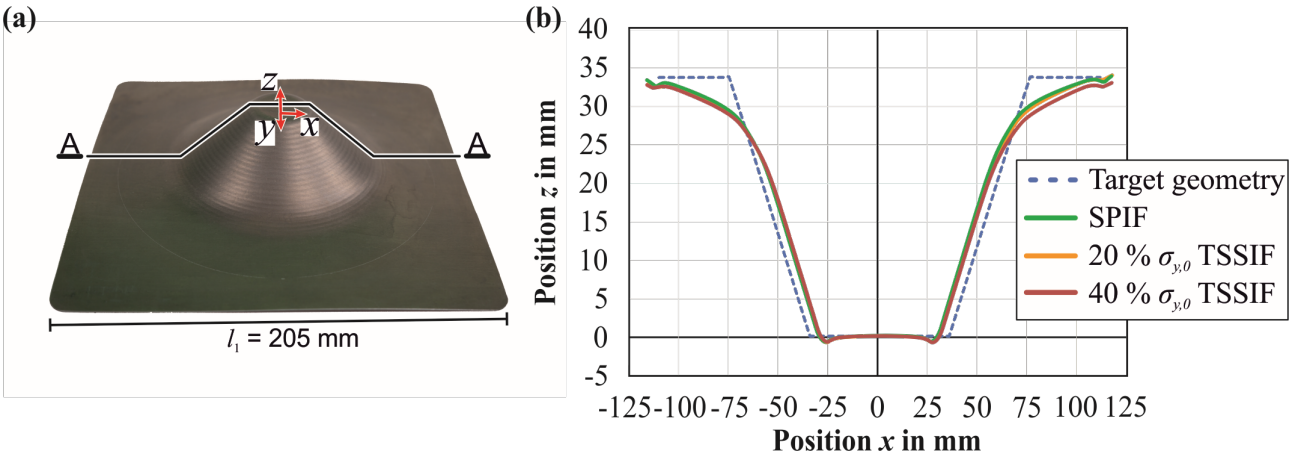

Figure 6. (a) Truncated cone geometry (b) Comparison of cut A-A cone geometries

Sheet thickness and material hardness. Sheet thickness and material hardness evaluation were performed at the location of the selected point (**Fig. 4b**). Stripes were extracted from this area in meridional direction and cold-mounted for microscopy.

The resulting sheet thickness evaluation is shown in **Fig. 7a**. Sheet thickness values are mean values of three repetitions. The initial thickness of the delivered AA 5083 material is t_0 = 0.97 mm. The sheet thickness reduction measured in the cone wall is almost equal comparing the three process variants. The resulting thickness is equal to the theoretical value ($t_{analytic}$ = 0.74 mm) calculated by sine-law for truncated cones with a wall angle $\Psi = 40°$.

The material hardness is measured in the cross section of the cone wall in the selected point using Vickers hardness HV0.3 (**Fig. 7b**). All hardness values are mean values of three measurements. The initial material hardness of the delivered AA5083 material is 74 ±3 HV0.3. After the forming processes, all specimens have a significantly higher material hardness between 114 and 116 HV0.3 in the forming zone compared to the initial material hardness. A comparison of the material harnesses of the process variants, point out no significant differences taken measurement scatter into account.

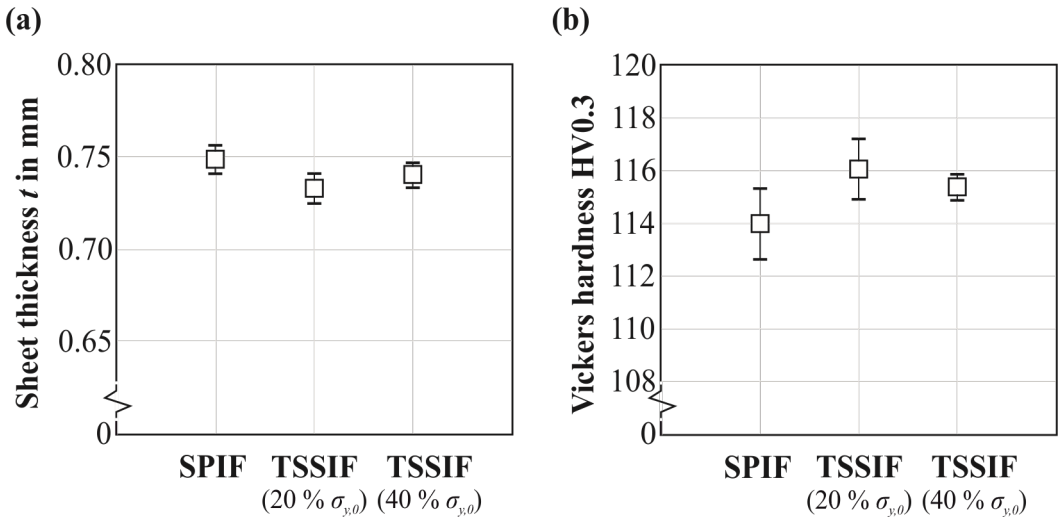

Figure 7. (a) Sheet thickness (b) Material hardness

Residual stress state. An evaluation of the experimental measured residual stresses located at the selected point of the cone wall (**Fig. 4b**) in meridional and circumferential direction on the tool side of the part (bottom-face) are shown in **Fig. 8**. The residual stress evaluation of the numerical model is located accordingly. The residual stresses in meridional direction on the bottom-face are tensile residual stresses (**Fig. 8a**). The residual stresses are monotonously increasing with increasing superposed tensile stress. The meridional residual stresses σ_m = 33 ±7 MPa are increased by 25 % for TSSIF with a tensile stress equal to 20 % of the initial yield stress and 49 % with a superposed tensile stress equal to 40 % of the initial yield stress. The residual stresses in circumferential direction on the bottom-face are monotonously increasing with increasing superposed tensile stress (**Fig. 8b**). The circumferential residual stresses σ_c = 42 ±11 MPa are increased by 47 % for TSSIF with a tensile stress equal to 20 % of the initial yield stress and 57 % with a superposed tensile stress equal to 40 % of the initial yield stress. The numerical results show the same behavior quantitatively and qualitatively.

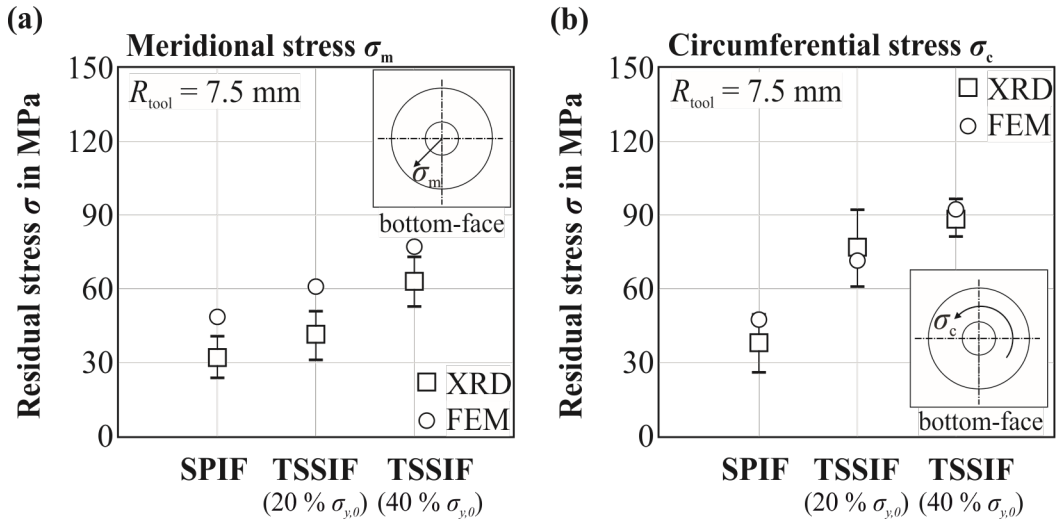

Figure 8. XRD results at the bottom-face (tool side) in (a) meridional direction and (b) circumferential direction

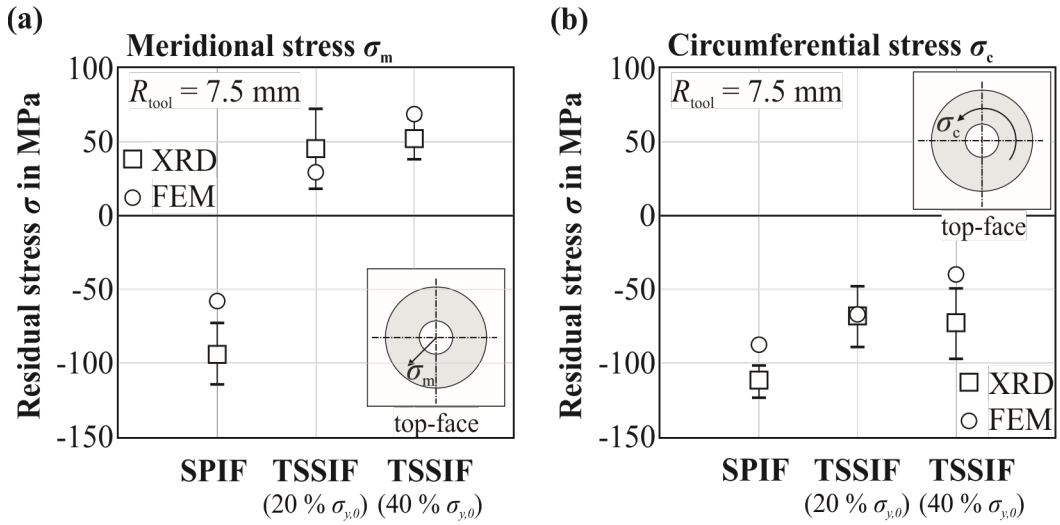

Figure 9. XRD results at the top-face (non-tool side) in (a) meridional direction and (b) circumferential direction

An evaluation of the residual stresses in meridional and circumferential direction on the non-tool side of the part (top-face) is shown in **Fig. 9**. The residual stresses in meridional direction on the top-face are compressive residual stresses for the SPIF process (**Fig. 9a**). The residual stresses are monotonously decreasing into the tensile range with increasing superposed tensile stress. The

meridional compressive residual stresses σ_m = -89 ±19 MPa are changed to tensile residual stresses for TSSIF. The compressive residual stresses in circumferential direction on the top-face are monotonously decreasing into the tensile range with increasing superposed tensile stress form σ_c = -112 ±11 MPa (**Fig. 9b**). The numerical results show the same behaviour quantitatively and qualitatively.

Discussion

A compassion of tensile stress superposed incremental formed AA 5083 cones with increasing biaxial tensile load in sheet plane direction and SPIF manufactured cones shows especially a difference regarding the residual stress state of the final cone geometry. The process force development and amplitudes of all process variants, with and without tensile stress-superposition, are on a similar level without significant differences in all three process force components. The thickness reduction in the cone wall of about 24% compared to the initial sheet thickness t_0 = 0.97 mm is similar in all considered process variants and according to the value that sine law predicts for cones with a wall angle of Ψ = 40°. The initial material hardness of the AA5083 material of 74 ±3 HV0.3 is increased by forming-induced hardening that leads to a final harness increase of 40 % in the cone wall. The final hardness of SPIF and TSSIF specimen are on the same level with small scattering. The cone geometry is only slightly affected by the tensile stress-superposition. There are small deviations in the flange region, but the relevant cone wall and bottom of the cone show no significant differences in geometry. The residual stress sate of the TSSIF cone specimens is significantly different than the SPIF cone specimens on both sides of the cone wall. It is observed, that increasing biaxial tensile stress shifts the residual stress state on both sides of the cone wall into the tensile stress region. Tensile stresses on the bottom-face of the cone are increased with increasing tensile stress-superposition. An initial tensile stress-superposition of 20 % of the initial AA5083 yield stress leads to 25 % higher tensile residual stress amplitudes in meridional direction σ_m on the bottom-face compared to the residual stresses σ_m = 33 ±7 MPa of the SPIF parts. Further increase of the initial tensile stress to 40 % of the initial yield stress leads to 74 % higher tensile residual stress amplitudes compared to the SPIF cones. For the residual stresses in circumferential direction σ_c a similar behavior can be observed. The change of residual stresses on the top-face is even higher due to generally higher compressive residual stress amplitudes compared to the tensile stress amplitudes on the bottom-face. High compressive residual stresses in meridional direction σ_m = -89 ±19 MPa on the top-face are shifted in tensile residual stresses with TSSIF. The tensile residual stress amplitude can be further increased by increasing tensile stress-superposition. Compressive residual stresses on the top-face stresses in circumferential direction σ_c that are measured for the SPIF cones are decreased with increasing initial tensile stress-superposition monotonously, but remain in the compressive region even for the highest initial tensile stress-superposition in this study. These findings show that a change of the initial stress state of the unformed sheet with small tensile stresses in the elastic range have a significant influence on the resulting residual stress state of the component. By analyzing the most relevant parameters, that can have an influence on the residual stresses of the components, it could be clarified that the initial stress state of the sheet is the most significant influence on the resulting residual stress state in this investigation.

Summary and Conclusion

A novel approach for tensile stress-superposed incremental forming (TSSIF) was introduced. The effect of TSSIF on the product properties was shown experimentally and numerically. A comparison of geometrically identical truncated cone geometries formed with SPIF and TSSIF demonstrated the capability of the novel approach. The superposition of small tensile stresses over the sheet plane to set the initial sheet's stress state has a significant effect on the residual stress state of the final component. By tensile stresses-superposition over the sheet plane in the elastic range of the material, the residual stress state of incremental formed cones could be shifted in the tensile residual stress region. With increasing initial tensile stresses-superposition, the decrease of compressive residual

stresses or increase of tensile residual stresses could be observed. Process forces were analyzed and showed no significant change by using TSSIF compared to SPIF process. Sheet thickness and material hardness was analyzed. Sheet thickness reduction and increased material hardening are noticed as described for SPIF processes. No influence of TSSIF on the sheet thickness or on the material hardness could be observed in this study. A comparison of the cone geometry showed a similarity for all investigated process variants with slight deviation in the flange area.

This knowledge can be used to set residual stresses in formed components for application-specific produce parts with localized properties. Further metallurgical analyzes regarding the grain structure and damage development need to be carried out to ensure these findings. Additionally, higher tensile loads should be tested with different materials to analyze the process limits.

Acknowledgements

The authors would like to thank the German Research Foundation (DFG, Deutsche Forschungsgemeinschaft) for funding the research project TE 508/67-3 part of the priority program SPP 2013 “The utilization of residual stresses induced by metal forming”.

Conflict of interest

The authors declare no conflict of interest.

References

[1] W.C. Emmens, A.H. van den Boogaard, An overview of stabilizing deformation mechanisms in incremental sheet forming, J. Mater. Process. Technol. 209 (2009) 3688–3695.

[2] P.A.F. Martins, N. Bay, M. Skjoedt, M.B. Silva, Theory of single point incremental forming, CIRP Ann. Manuf. Technol. 57 (2009) 247–252.

[3] E. Leszak, Apparatus and process for incremental dieless forming, U.S. Patent 3342051A1. (1967)

[4] J. Jeswiet, E. Hagan, Rapid proto-typing of a headlight with sheet metal, Proceedings of Shemet, 2001, pp. 165–170.

[5] N.N. Powell, C. Andrew, Incremental forming of flanged sheet metal components without dedicated dies, Proceedings of the Institution of Mechanical Engineers, Part B: J. Eng. Manuf. 206 (1992) 41–47.

[6] B. Taleb Araghi, G.L. Manco, M. Bambach, G. Hirt, Investigation into a new hybrid forming process: Incremental sheet forming combined with stretch forming, CIRP Annals 58 (2009) 225–228.

[7] F. Maqbool, F. Maaß, J. Buhl, R. Hajavifard, F. Walther, A.E. Tekkaya, M. Bambach, Targeted residual stress generation in single and two point incremental sheet forming (ISF), Arch. Appl. Mech. 91 (2021) 3465–3487.

[8] F. Maaß, M. Hahn, A.E. Tekkaya, Adjusting residual stresses by flexible stress superposition in incremental sheet metal forming, Arch. Appl. Mech. 91 (2021) 3489–3499.

[9] E. Macherauch, P. Müller, Das $\sin^2\Psi$-Verfahren von röntgenographischen Eigenspannungen, Zeitschrift für angewandte Physik 13 (1961) 305–312.

[10] J. Lemaitre, J.-L. Chaboche, Mechanics of solid materials, Cambridge University Press, Cambridge, 2012.

[11] F. Maaß, M. Hahn, A.E. Tekkaya, Interaction of process parameters, forming mechanisms and residual stresses in Single Point Incremental Forming, Metals 10 (2020) 656.